

The values for palladium measured by Eichenhauer and Schäfer⁴ lie between those of reference 3 and ours.

We have also measured the specific heat of a polycrystalline sample of vanadium metal carefully and confirm the result of Clusius, Franzosini, and Piesbergen,⁸ who also made closely spaced measurements, that no appreciable anomaly in specific heat exists in vanadium between 175° and 265°K. Burger and Taylor⁹ reported small anomalies in the magnetic susceptibility and in the electrical resistivity of pure vanadium, which they associated with a possible antiferromagnetic structure.

¹F. E. Hoare and J. C. Matthews, Proc. Roy. Soc. (London) A212, 137 (1952).

²A. B. Lidiard, Proc. Roy. Soc. (London) A224, 161 (1954).

³K. Clusius and L. Schachinger, Z. Naturforsch. 2A, 90 (1947).

⁴W. Eichenhauer and L. Schäfer, Z. Naturforsch. 11A, 955 (1956).

⁵R. H. Beaumont, H. Chihara, and J. A. Morrison, Phil. Mag. 5, 188 (1960).

⁶C. H. Shomate, J. Chem. Phys. 13, 326 (1945).

⁷K. K. Kelley, J. Chem. Phys. 11, 16 (1943).

⁸K. Clusius, P. Franzosini, and U. Piesbergen, Z. Naturforsch. 15A, 728 (1960).

⁹J. P. Burger and M. A. Taylor, Phys. Rev. Letters 6, 185 (1961).

CURRENT SATURATION IN PIEZOELECTRIC SEMICONDUCTORS

Roland W. Smith

RCA Laboratories, Princeton, New Jersey

(Received June 13, 1962)

The dark current in semiconducting CdS, $\sigma \sim 0.1 (\Omega \cdot \text{cm})^{-1}$, saturates at an applied electric field ~ 1600 volts/cm. The drift velocity of electrons of $\mu \sim 300 \text{ cm}^2/\text{volt sec}$ in this field is $\sim 5 \times 10^5 \text{ cm/sec}$. The current then saturates when the drift velocity of electrons is comparable with the velocity of sound in the crystal. Hutson, McFee, and White¹ recently demonstrated ultrasonic amplification in photoconductive CdS, when the drift velocity of electrons exceeds the velocity of sound in the crystal. We believe that the current saturation reported here arises from the saturation of drift velocity of electrons due to energy transfer from the electron stream to a traveling wave of phonons in the piezoelectric crystal.

Figure 1 shows a typical $V-I$ characteristic for a $0.1 (\Omega \cdot \text{cm})^{-1}$ CdS crystal with the electric field parallel to the c axis. The curve was obtained with voltage pulses $10 \mu\text{sec}$ long. Ohmic contacts of both In and Ga have been used. Saturation is obtained with both vapor-phase-grown platelets and with sections cut from a large boule of CdS. For platelet crystals saturation is direction sensitive as follows:

(a) Stable saturation is always obtained with $E \parallel c$ when $E \sim 1600$ volts/cm.

(b) Saturation can also be obtained with $E \perp c$ and with current flow through the thin section of the crystal when $E \sim 1600$ volts/cm.

(c) The hard saturation shown in Fig. 1 is not

apparent with $E \perp c$ and current flow along the length of crystal. The Ohm's-law current is well behaved below $E \sim 1600$ volts/cm. Above this field there is evidence for incipient saturation, but the current becomes erratic and the higher the voltage is pushed the more likely it is that the crystal will "break down," i.e., become open-circuited and visibly damaged. In any case if saturation can be obtained it is at a field $>1600 \text{ V/cm}$, the current is less stable, and prolonged operation is not possible.²

Saturation is obtained with ease in the c direction of CdS needles, and is also obtained with CdSe at a slightly lower field. We have also

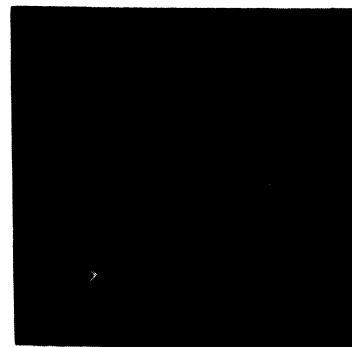


FIG. 1. $V-I$ characteristic for CdS. $L = 0.05 \text{ cm}$, $W = 0.025 \text{ cm}$, $T = 6 \times 10^{-3} \text{ cm}$. $V = 20 \text{ volts/div}$ (horizontal), $I = 5 \text{ mA/div}$ (vertical). $I \parallel c$ axis.

observed saturation in GaAs at 80 volts/cm with $E \parallel [111]$. Saturation should not be obtained with $E \parallel [100]$. The case GaAs is being checked more extensively.

The saturation described above has its origin in the body of the crystal and is not associated with contact phenomenon, other than the requirement that the contacts be Ohmic. The following data support this conclusion:

1. Potential probe measurements along the surface of the crystal show (a) that the potential drop at any point is essentially proportional to the applied voltage, including the saturation region, and (b) that the potential drop at any point varies linearly with distance along the crystal. The potential drop, as revealed by a probe, is not localized at either electrode, and does not shift distribution with applied voltage.

2. In some cases photocurrent several times the dark current can be obtained with saturation setting in at essentially the same field as for the dark current. In other words the contact can meet the demands of increased conductivity, and was therefore Ohmic.

3. With 20 pulses/sec no change in $V-I$ characteristic was noted for pulse lengths up to $\sim 200 \mu\text{sec}$, and similarly 10- μsec pulses up to ~ 200 pulses/sec produced no change. The extremely wide range over which the $V-I$ curve is independent of dissipation rate eliminates thermal heating from the saturation mechanism.

4. Table I summarizes data on resistance, maximum saturation current, ratio of resistance and ratio of maximum saturation current, and saturation threshold field for three different temperatures. It is apparent from these data that saturation cannot be due to temperature-limited emission from the cathode.

5. The conductivity between two small electrodes across the center of a platelet and trans-

verse to the current path was monitored while the main voltage pulses were applied along the length of the crystal. Although some change in conductivity was observed when the crystal was operated in the saturation region, the change in transverse conductivity was small compared with the corresponding change in longitudinal conductivity. This observation is consistent with saturation of longitudinal drift velocity, while the transverse drift velocity and density remain independent of the applied voltage. In a corollary experiment, a small 10^6 -cps signal applied along the direction of current flow was strongly attenuated when the main pulse along the crystal was in the saturation region.

6. The onset of saturation was observed with nanosecond rise time voltage pulses. In the Ohm's-law region the current immediately rises to a steady value determined by the voltage. The shape of the current pulse changes dramatically as the voltage rounds the knee of the saturation curve. For the first 50-100 nsec the current is constant and equal to its (extrapolated) Ohm's-law value. Subsequently the current decays to the final saturation value. The significant features of this behavior are shown in Fig. 2 for a crystal in which the long oscillatory decay to saturation is especially pronounced. The amplitude and shape of the decay transient varies from crystal to crystal. The oscillations are definitely associated with the crystal and are not due to a spurious circuit effect. It appears reasonable that the oscillations seen here are related to the response of the piezoelectric crystal to shock excitation. The frequency of the oscillations, ~ 2 Mc/sec, is about what would be expected from exciting the fundamental mode between the electrodes spaced 0.5 mm apart. While this acoustic frequency is not believed to be responsible for saturating the

Table I. Summary of $V-I$ data for CdS at three different temperatures.

(°K)	Resistance (k Ω)	I (sat.) (mA)	Ratio	$E_{\text{sat.}}$ (V/cm)	
373	2.7	37	$\frac{R(300)}{R(375)} = 0.9$	$\frac{I_{\text{sat.}}(373)}{I_{\text{sat.}}(300)} = 1.06$	2000
300	2.4	35			1600
77	16	6	$\frac{R(77)}{R(300)} = 6.6$	$\frac{I_{\text{sat.}}(300)}{I_{\text{sat.}}(77)} = 5.8$	2600

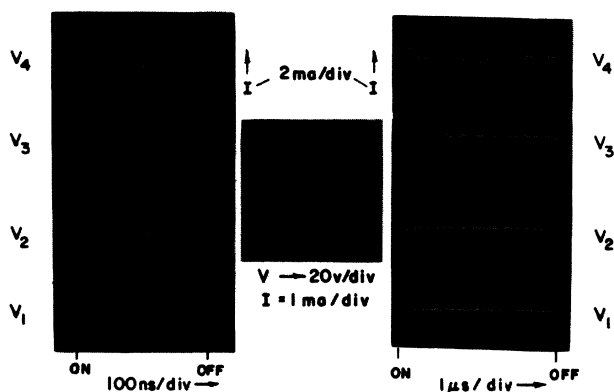


FIG. 2. Time dependence of current for dc voltage pulses. V_1 corresponds to a voltage just below the knee of the $V-I$ curve, while V_2 , V_3 , and V_4 correspond to increasing increments in voltage going over the knee. Left: Current pulses due to 1-nsec rise time voltage pulses; decay time of voltage pulse ~ 100 nsec. Center: $V-I$ characteristic. Right: Current pulses due to essentially equivalent amplitude voltage pulses as left curves but of $10 \mu\text{sec}$ duration. Voltage pulse rise time here ~ 30 nsec. Pulse repetition rate ~ 60 pulses/sec in both cases.

current, it is, nevertheless, significant that the ringing of this mode is prolonged by operating over the knee of the curve, indicating absorption of energy from the dc current.

The $V-I$ characteristic is not detectably altered by a magnetic field up to ~ 7000 oersteds. The conductivity of normally insulating CdS can be brought into the semiconducting range by light. In this conductivity range the photocurrent saturates just as in the case with semiconducting crystals. The saturation threshold field is also ~ 1600 V/cm when the photoconductivity is $\sim 0.01 (\Omega\text{-cm})^{-1}$. As the photocurrent is lowered the saturation knee broadens, and at still lower levels the current is completely Ohmic (Fig. 3). The saturated photocurrent reported here undoubtedly corresponds to the conditions obtaining in the Hutson, McFee, and White experiments¹ when ultrasonic gain is observed.

The following mechanism is proposed for the current saturation described above.³ When the drift velocity of electrons exceeds the velocity of sound, acoustic waves in the crystal gain energy from the field and a growing hypersonic wave is generated. If the amplitude of the sound wave is sufficiently large, the potential difference between crest and trough will exceed kT/e , and substantially all of the free carriers will be bunched in the potential troughs, and the local

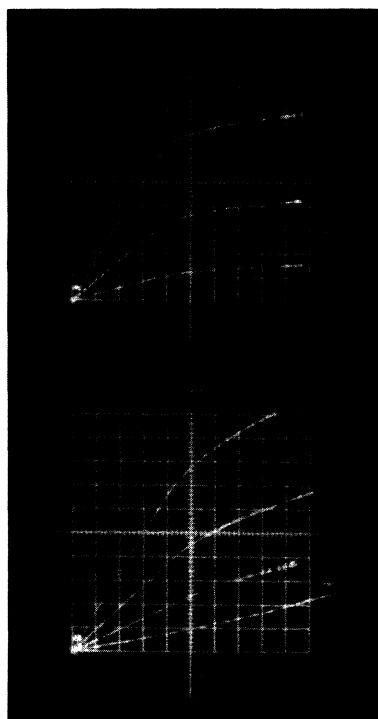


FIG. 3. $V-I$ characteristic for photocurrent. Top curve $I = 5$ mA/div, bottom curve $I = 0.15$ mA/div. 20 volts/div, for both curves (horizontal). $L = 0.05$, $W = 0.03$, $T = 5 \times 10^{-3}$ cm. Note total change in resistance is 280:1.

piezoelectric fields will exceed the applied field. Increasing the electric field under these conditions will push the electrons harder against the walls of their potential troughs and will increase the power going into the sound wave without causing the electrons to drift faster than the sound wave. Hence in this range of fields the current is saturated and the extra power is absorbed in the hypersonic wave. From the relation for gain given by Hutson *et al.*,¹ one would expect the maximum gain to occur for phonon frequencies between $\omega_D \sim 10^{10}$ and $\omega_C \sim 10^{12} \sigma$,⁴ where the gain/cm can exceed 10^3 dB and be sufficient to generate the large-amplitude acoustic waves needed to saturate the current. In our experiments σ ranges from 0.01 to $3 (\Omega\text{-cm})^{-1}$. Hence, the phonons selected out for preferential amplification should be in the gigacycle range. Phonon-phonon scattering may also set the upper limit (for $T > 50^\circ\text{K}$) in the gigacycle range.^{5,6} Several attempts to detect either the hypersonic waves or electromagnetic radiation from the bunched electrons have been unsuccessful.

Hutson *et al.*¹ describe the amplification of shear waves only. The fact that we obtain saturation along the c direction for plates and needles means, according to Hutson's analysis,⁷ that we are amplifying longitudinal waves.

The mechanism for saturation proposed here is due to A. Rose. The author wishes to thank A. Rose, M. Lampert, D. O. North, and other colleagues in the General Solid State Research Group for stimulating discussions and valuable suggestions. C. Oldakowski was most helpful with the experiments, the fast pulse experiments were made with the help and cooperation of R. Shahbender, and the first $V-I$ curves were obtained with R. Larrabee's equipment.

¹A. R. Hutson, J. H. McFee, and D. L. White, Phys. Rev. Letters **7**, 237 (1961).

² $E \parallel c$ should excite longitudinal hypersonic waves in the crystal. $E \perp c$ should excite shear waves. In case

(c) the shear waves vibrate along the easy cleavage direction of the platelet.

³During the course of this work the strong interaction between electronic currents and acoustic waves expected from the analysis by Hutson, McFee, and White was reported by L. Esaki [Phys. Rev. Letters **8**, 4 (1962)] for bismuth. Since Esaki's currents were two-carrier currents, the saturation effect reported here could not be observed. Rather, a strong interaction between Hall currents and acoustic waves gave rise to an effectively shorter collision time for the carriers and a decreased magnetoresistive effect. W. P. Dumke and R. R. Haering [Phys. Rev. **126**, 1974 (1962)] and J. J. Hopfield [Phys. Rev. Letters **8**, 311 (1962)] treat this model in more detail.

⁴ $\omega_c = \sigma/\epsilon$, the conductivity relaxation frequency, $\omega_D = v^2/D$, where v = the velocity of sound, and D = the carrier diffusion constant.

⁵H. E. Bömmel and K. Dransfeld, Phys. Rev. Letters **2**, 298 (1959).

⁶H. D. Nine and R. Truell, Phys. Rev. **123**, 801 (1961).

⁷A. R. Huston and D. L. White, J. Appl. Phys. **33**, 45 (1962).

MAGNETIC ORDERING AND THE ELECTRONIC STRUCTURE OF RARE-EARTH METALS*

A. R. Mackintosh

Institute for Atomic Research and Department of Physics, Iowa State University, Ames, Iowa
(Received March 19, 1962; revised manuscript received June 1, 1962)

The available experimental evidence, particularly the data on the entropy and the magnetic properties,¹ indicates that the outer electrons in the rare-earth metals can be classified into two groups: localized $4f$ electrons, with an unquenched orbital moment, and conduction electrons. Some of the electronic properties of the rare-earth metals have been interpreted by the author,² using a model in which the localized electrons are described by atomic $4f$ wave functions, and the conduction electrons are treated as almost free. The purpose of this note is to emphasize the effect that the magnetic ordering of the localized electrons can have on the Brillouin zone structure, and hence on the conduction electrons.

It is known³ that, below characteristic transition temperatures, the rare earths are magnetically ordered. In particular, there exist antiferromagnetic phases with a periodic arrangement of magnetic moments along the c axis, with a period, in general, incommensurate with that of the lattice. This arrangement may be a spiral, a sinusoidal variation of magnetic moments, or some more complex structure. The extra periodicity along

the c axis can introduce extra planes of energy discontinuity into the Brillouin zone structure by two mechanisms:

(a) The exchange interaction between the localized and conduction electrons, which takes the form

$$H_{1c} = K(g-1)\vec{J}_1 \cdot \vec{s}_c, \quad (1)$$

where K is an effective exchange integral, g the Landé factor for the ionic moment \vec{J}_1 , and where \vec{s}_c , the conduction electron spin, depends on the orientation of the localized moments. If, therefore, we have a periodic variation of the ionic moments along the c axis, as shown in Fig. 1(a), the electron wave functions (1) and (11), which have the same wavelength, have different energy eigenvalues. The effect on the Brillouin zone structure is shown in Fig. 1(b), where the dotted lines represent extra planes of energy discontinuity due to the magnetic superlattice. From the magnetic transition temperatures and experiments on the scattering of conduction electrons by rare-earth impurities,⁴ we estimate these energy gaps to be of the order of 0.5 eV. This type of mechanism

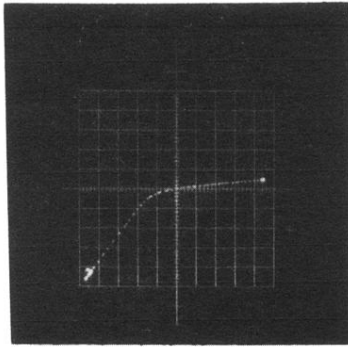


FIG. 1. $V-I$ characteristic for CdS. $L = 0.05$ cm, $W = 0.025$ cm, $T = 6 \times 10^{-3}$ cm. $V = 20$ volts/div (horizontal), $I = 5$ mA/div (vertical). $L \parallel c$ axis.

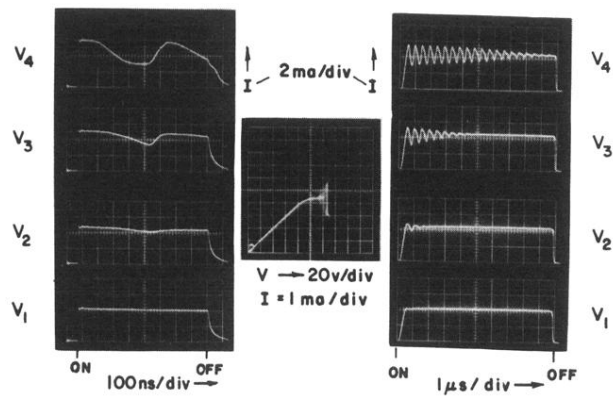


FIG. 2. Time dependence of current for dc voltage pulses. V_1 corresponds to a voltage just below the knee of the $V-I$ curve, while V_2 , V_3 , and V_4 correspond to increasing increments in voltage going over the knee. Left: Current pulses due to 1-nsec rise time voltage pulses; decay time of voltage pulse ~ 100 nsec. Center: $V-I$ characteristic. Right: Current pulses due to essentially equivalent amplitude voltage pulses as left curves but of $10 \mu\text{sec}$ duration. Voltage pulse rise time here ~ 30 nsec. Pulse repetition rate ~ 60 pulses/sec in both cases.

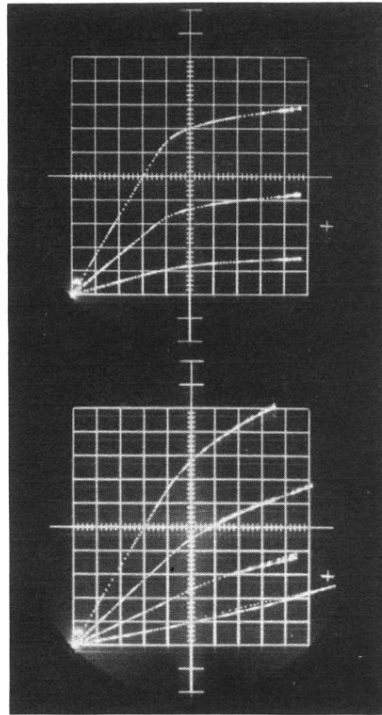


FIG. 3. $V-I$ characteristic for photocurrent. Top curve $I=5$ mA/div, bottom curve $I=0.15$ mA/div. 20 volts/div, for both curves (horizontal). $L=0.05$, $W=0.03$, $T=5 \times 10^{-3}$ cm. Note total change in resistance is 280:1.